RSC Advances

PAPER

View Article Online
View Journal | View Issue

Cite this: *RSC Adv.*, 2016, **6**, 7061

Hydroxylated fullerene-capped, vinblastine-loaded folic acid-functionalized mesoporous silica nanoparticles for targeted anticancer therapy†

Nikola Ž. Knežević,*[a] Jasminka Mrđanović,[b] Ivana Borišev,[c] Sanja Milenković,[c] Đorđe Janaćković,[a] Frédérique Cunin[d] and Aleksandar Djordjevic[c]

Received 1st November 2015
Accepted 8th January 2016

DOI: 10.1039/c5ra22937e

www.rsc.org/advances

A novel cancer-targeting drug delivery system is constructed and characterized, based on folic acid-functionalized mesoporous silica nanoparticles with pore-loaded anticancer drug vinblastine and pore-blocking fullerenol molecules. The selective treatment efficacy based on targeting of cancer-overexpressed folate receptors is demonstrated by comparison of cell viability upon the treatment of healthy MRC-5, breast cancer MCF-7 and cervical cancer HeLa cells, which are known to differ in the amount of folate receptors on their surfaces.

Introduction

One of the most important aspects in the use of nanoparticles as drug delivery carriers is the opportunity to target the drug activity to a desired treatment area. A variety of specific receptors have been identified as markers for targeting nanotherapeutics to cancer tissues, cells or even specific organelles within them.[1] Among them folate receptors (FR) are particularly known for their overexpression in many cancers, with the highest frequency (>90%) in ovarian carcinomas.[2] In addition, FR-targeted cancer therapy is appealing because of the high folate-FR binding constant, low immunogenicity, ease of surface functionalization with folate molecules, increased FR density in more advanced cancers, and even in cases when FR are expressed by normal tissues, they are typically unreachable for folate-functionalized drug carriers until malignant transformation occurs.[3]

Mesoporous silica nanoparticles (MSN),[4–7] and analogous silica-based nanocarriers like *e.g.* halloysite nanotubes,[8] have been at the forefront of research efforts for the past decade as the scaffold for constructing multipurpose nanotherapeutics. Suitability of MSN for this purpose is ensured by small particle diameters, high surface areas, stable mesoporous morphologies, easiness of surface functionalizations and high biocompatibility. Biodegradability studies of MSN-based drug delivery systems showed that, in case of *in vitro* experiments, their intracellular degradation completes within 3 weeks of the treatment.[9] *In vivo* studies on mice revealed that these nanomaterials are not cytotoxic, capable to selectively target cancer tissue and to excrete through renal and urinary pathways.[10,11] Typically, drugs are loaded inside the mesopores of MSN and their retention is ensured by the presence of pore-capping moieties, which therefore assist in delivering high amounts of drugs to the treatment areas. A variety of simple to highly complex concepts have been demonstrated for this application.[12] However, up until our recent study,[13] there were no reports on application of fullerene-based molecules for serving as pore blockers in constructing drug delivery systems from porous silicate nanomaterials. Hydroxylated fullerenes (fullerenols, $C_{60}(OH)_n$) are known for their beneficial properties in biological applications such as the ability to reduce side-effects of cytotoxic drugs,[14,15] applicability in photothermal therapy (PTT) and imaging of cancer,[16] as radioprotectors,[17] for construction of fullerenol-conjugates for cancer therapy,[18] as well as the capability for light responsive formation of reactive oxygen species (ROS).[19] In aqueous solutions hydroxylated fullerenes are known to self-assemble into clusters, *i.e.* fullerenol nanoparticles (FNPs), which have been also shown to reduce the health hazard of toxic molecules.[20] All of these attributes of hydroxylated fullerene may be exploited in the future to construct multipurpose fullerenol or FNP-containing nanocomposites, *e.g.* drug delivery systems for simultaneous imaging and cancer therapy through targeted drug delivery, PTT and photodynamic therapy.

We previously demonstrated that hydroxylated fullerene can be indeed efficiently applied for entrapping cargo drug

[a]*Faculty of Technology and Metallurgy, University of Belgrade, Karnegijeva 4, 11000 Belgrade, Serbia. E-mail: nikola.z.knezevic@gmail.com*

[b]*Oncology Institute of Vojvodina, Faculty of Medicine, University of Novi Sad, Put Dr Goldmana 4, 21204 Sremska Kamenica, Serbia*

[c]*Faculty of Science, Department of Chemistry, Biochemistry and Environmental Protection, University of Novi Sad, Trg Dositeja Obradovića 3, 21000 Novi Sad, Serbia*

[d]*Institut Charles Gerhardt Montpellier, UMR 5253 CNRS-ENSCM-UM2-UM1, Ecole Nationale Supérieure de Chimie de Montpellier, 8 rue de l'Ecole Normale, 34296 Montpellier, France*

† Electronic supplementary information (ESI) available: TEM images, synthesis of FNP@FAMSN and VIN@FAMSN, low angle XRD and fluorescence measurements, viability study results with FNP@FAMSN. See DOI: 10.1039/c5ra22937e

(9-aminoacridine) inside the porous silica nanoparticles,[13] and capping of micropores of the material was found to be prevalent in comparison to the capping of mesopores. The release of higher amounts of the drug was also noted upon acidification of the environment which is beneficial from the standpoint of selectivity of cancer treatment, as pH values in tumour tissues are lower in comparison to healthy tissues.[21] Herein we further report on the applicability of fullerenol for construction of more complex MSN-based cancer-targeting nanotherapeutics. Anticancer drug vinblastine (VIN) is loaded in folic acid-functionalized MSN (FAMSN) and we showcase that fullerenol ($C_{60}(OH)_{24}$) can be utilized for the effective capping of the mesopores of the material as well, to entrap the anticancer drug (Scheme 1). The constructed material is then investigated for application in FR-targeted anticancer treatment by *in vitro* studies against one healthy and two malignant cell lines, which are known to contain different amounts of expressed FR.

Experimental

Hexadecyltrimethylammonium bromide (CTAB), tetraethyl orthosilicate (TEOS), 3-aminopropylltriethoxysilane (APTES), fullerene C_{60}, folic acid (FA), dicyclohexylcarbodiimide (DCC) and vinblastine (VIN) were commercially available (Sigma-Aldrich). Fullerenol nanoparticles ($C_{60}(OH)_{24}$) were synthesized according to the previously published procedure from fullerene-C_{60} through catalytic bromination,[22] followed by substitution of bromide with hydroxyl groups.[23]

Instruments and methods

Infrared spectra were collected on Thermo Nicolet Nexus 670 FTIR spectrometer, UV/VIS measurements were performed on Scientific Equipment Cintra 1010. Thermogravimetric analysis (TGA) was done on TA instrument SDT Q600 up to 800 °C in air with a heating rate 20 °C min^{-1}. Transmission electron micrographs (TEM) were obtained on JEOL 1200 EXII instrument. Low angle XRD measurements were carried out on Bruker AXS D8 XRD – diffractometer. Fluorescence measurements were performed on Perkin Elmer LS45 fluorescence spectrometer. The specific surface areas and pore size distribution of the samples were estimated using nitrogen adsorption–desorption isotherms with Micrometrics ASAP 2020 instrument. Before the sorption measurement, samples were degassed at 105 °C for 10 h under reduced pressure. The specific surface area of sample (S_{BET}) was calculated according to the Brunauer, Emmett, Teller (BET) method from the linear part of the nitrogen adsorption isotherm. Volume of the mesopores and pore size distribution were analyzed according to the Barrett, Joyner and Halenda (BJH) method.

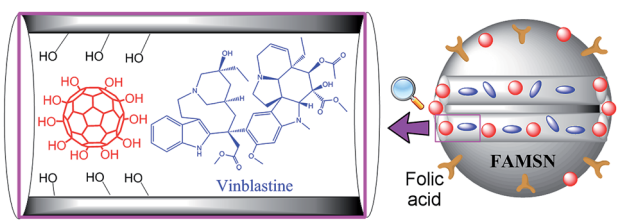

Scheme 1 Depiction of encapsulation of vinblastine inside the mesopores of FAMSN by the presence of hydroxylated fullerenes.

Synthesis of folic acid functionalized mesoporous silica nanoparticles (FAMSN)

Solution of CTAB (1.00 g, 2.74 mmol) and NaOH (aq.) (2.00 mol L^{-1}, 3.50 mL) in 480 mL of demineralized water was prepared, followed by adjusting the solution temperature to 80 °C. TEOS (5.00 mL, 21.9 mmol) was introduced dropwise to the solution and the mixture was allowed to stir for 2 h, giving rise to white precipitate (as-synthesized MSN). The solid product was filtered through a sintered glass funnel, washed with demineralized water and MeOH, and dried in air over night. This material (MSN) was further used for functionalization of the external surface (before removal of the surfactant template) with folic acid in the following manner: folic acid 0.4550 g (0.001 mol), DCC 0.2063 g (0.001 mol) and 0.18 mL of APTES (0.001 mol) were dissolved in 30 mL of dry DMSO and stirred for 24 h at room temperature under nitrogen. The reaction mixture was than filtered, filtrate was added to 1 g of MSN and the suspension was refluxed for 4 h at 110 °C. The solid product was filtered through a sintered glass funnel, washed with copious amount of demineralized water and methanol, and dried in air over night. Removal of the CTAB surfactant template was then performed by heating at 60 °C for 6 h in a solution of HCl in methanol (1%, v/v). After the surfactant extraction, the material was additionally washed with copious amount of demineralized water and methanol, and dried in air.

Preparation of vinblastine-loaded, fullerenol-capped FAMSN material (FNP-VIN@FAMSN)

Fullerenol (5.0 mg) was measured in a 100 mL flask and 50 mL of phosphate buffer (pH 7.4) was added. The solution was sonicated for 10 min and stirred over night at room temperature in order to fully dissolve FNPs. In a second flask containing 2.0 mL (1 mg mL^{-1}, 2.1 μmol) of vinblastine sulfate in demineralized water, 3 mL of PBS buffer was added (10 mM, pH 7.4), followed by addition of 100 mg FAMSN. The mixture was stirred at room temperature for 24 h and then the solution of FNP in PBS was added. After additional stirring at room temperature for 20 h suspension was centrifuged at 8000 rpm for 15 min, washed with PBS buffer, water and ethanol and dried at 80 °C. The filtrate was saved for determination of the drug loading.

The amount of loaded drug was determined by the standard curve method. Namely, the standard curve was prepared by measuring UV/VIS absorption of 5 different concentrations of VIN in ethanol at 267 nm. The filtrate obtained after the drug loading and capping with FNP was collected and the solvents were evaporated. VIN was then dissolved in ethanol and the UV/VIS absorbance of the solution was measured at 267 nm for determination of VIN concentration from the standard curve. This procedure was performed in order to eliminate the

influence of absorption of FNP from the filtrate at 267 nm since it is insoluble in ethanol. The calculated amount of leftover drug was 0.7 μmol, which gave the amount of loaded drug (1.4 μmol/100 mg of FAMSN) by subtraction from the starting 2.1 μmol of VIN.

Determination of release kinetics of the drug from FNP-VIN@FAMSN

A vial containing 10 mg of FNP-VIN@FAMSN in 5 mL of PBS was prepared and the suspension was left stirring at room temperature. Aliquots were taken from the suspension at designated times after which the suspensions were centrifuged for 10 min at 14 000 rpm, the supernatants were evaporated to dryness and VIN was dissolved in ethanol. UV/VIS absorbance of released VIN was then measured at 267 nm.

Cell cultures

The MRC-5, MCF-7 and HeLa cell lines were cultured in 25 mL flasks (Costar, USA) in 10 mL of DMEM medium, supplemented with 2 mL L-glutamine, 10% FCS, 100 IU mL^{-1} penicillin, and 100 μg mL^{-1} streptomycin at 37 °C in a fully humidified atmosphere with 5% CO_2. Confluent cells were detached with 0.25% trypsin and 0.05% EDTA for 3 min, and aliquots of cells were sub-cultured. Cell growth was evaluated by colorimetric sulforhodamine B (SRB) assay.[24] The MRC-5, MCF-7 and HeLa cell lines were harvested and plated into 96-well microtiter plates (Sarstedt, Newton, USA) at 10×10^3 cells per well seeding density in a volume of 180 μl, in DMEM medium supplemented with 5% FCS, at 37 °C.

After 24 h of preincubation, the cells were treated in octuplicate with FNP-VIN@FAMSN and FNP@FAMSN at 6.25, 12.5, and 25 μg ml^{-1} concentrations, while the control cells were treated only with 20 μl of DMEM. After 24 h of the incubation at 37 °C/5% CO_2, the cells were fixed with 50% TCA (1 h, +4 °C), washed with distilled water (Wellwash 4, Labsystems; Helsinki, Finland) and stained with 0.4% SRB (30 min, room temperature). The plates were then washed with 1% acetic acid to remove unbound dye. Protein-bound dye was extracted with 10 mM TRIS base. Absorbances were measured on a microplatereader (Multiscan Ascent, Labsystems; Helsinki, Finland) at 540/620 nm.

Results and discussion

Mesoporous silica nanoparticles were prepared by surfactant-templated synthesis,[25] by condensation of silicate precursors in basic aqueous solution. External surface modification with folic acid was achieved by carbodiimide activated amidation of folic acid with APTES and *in situ* surface grafting on surfactant-containing MSN. Removal of the surfactant was performed by refluxing the suspension of the material in acidic methanol solution (1 wt%). FTIR spectrum of the material (Fig. 1a) reveals the presence of organic functional groups on the material's surface. Stretching C–H vibrations are evident at the wavenumber around 3000 cm^{-1}, vibration band at 1703 cm^{-1} points to carboxylic acid group while bands

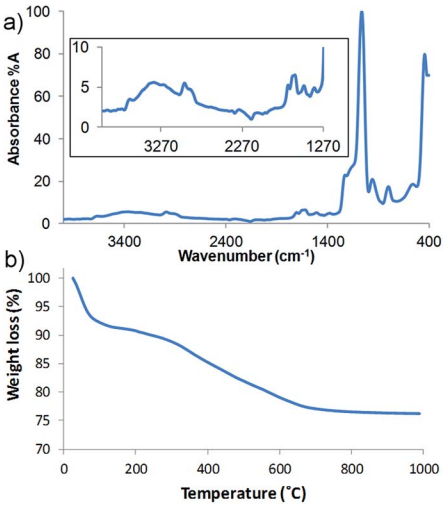

Fig. 1 Characterization of FAMSN material by (a) FTIR spectroscopy and (b) thermogravimetric analysis (TGA).

at 1640 and 1620 cm^{-1} can be ascribed to vibrations of different amide moieties of the surface functionalized molecule. Aromatic C–C vibrations are evident at 1506 cm^{-1} and aliphatic at 1377 cm^{-1}. The broad band at around 1100 cm^{-1} arises from various Si–O stretching vibrations of the silicate material. The amount of functionalized organic moieties was determined (14 wt%) from TGA analysis of the FAMSN after accounting for 9 wt% of adsorbed water which is lost upon heating by 130 °C (Fig. 1b). Transmission electron micrographs (TEM) of FAMSN (Fig. 2a) reveal spherical morphology and mesoporous texture of the nanoparticles, with particle diameters in the range: 60–200 nm. After the addition of FNP, the presence of brighter FNP clusters (*ca.* 10 nm) is clearly visible on the surface of MSN (Fig. 2b–d, Fig. S1†).

As a comparison, TEM images of vinblastine loaded FAMSN (VIN@FAMSN) and fullerenol loaded FAMSN (FNP@FAMSN) are provided on Fig. S2.† As evident, the uniform FNP clusters are absent in these images, which points to the role of vinblastine in establishing the clustered morphology of FNP-VIN@FAMSN, probably through hydrogen bonding between VIN and fullerenols. Nitrogen sorption measurements revealed

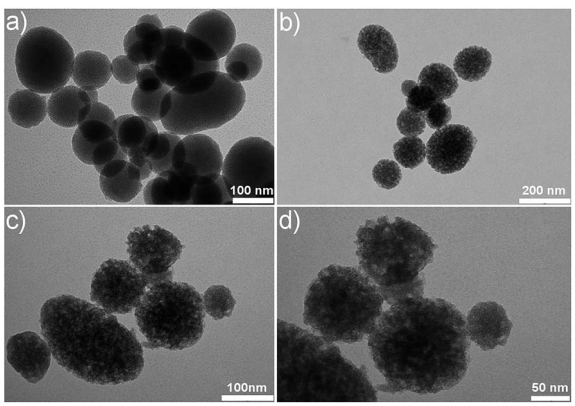

Fig. 2 TEM images of: (a) FAMSN and (b–d) FNP-VIN@FAMSN.

that fullerenol molecules were also capable to enter the mesopores since the shape of BET isotherm changed from type IV for FAMSN, which is typical for mesoporous materials, to type II for FNP-VIN@FAMSN (Fig. 3a). This result evidences the obstruction of uniform capillary condensation of nitrogen, as observed for FAMSN, inside the mesopores due to the presence of bulky fullerenol in FNP-VIN@FAMSN. This change is also followed by the decrease in BET surface area from 658 $m^2 g^{-1}$ (for FAMSN) to 426 $m^2 g^{-1}$ (FNP-VIN@FAMSN). BJH calculations (Fig. 3b) demonstrate that FAMSN contains prevailing 2.2 nm-sized diameter of mesopores that are not detected in FNP-VIN@FAMSN, which further supports the mesopore-capping ability of fullerenol. Low angle XRD measurements also evidence the capability of fullerenol to obstruct the pores of FAMSN since the (100) peak disappears in case of the materials containing fullerenol (FNP-VIN@FAMSN and FNP@FAMSN) (Fig. S3†).

Release kinetics of the encapsulated drug was determined by dispersing FNP-VIN@FAMSN in PBS buffer (2 mg mL^{-1}) and by measuring VIN concentration in the bulk solution over time. The aliquots were first subjected to centrifugation to remove the suspended material, followed by evaporation of the supernatants to dryness and extraction of vinblastine with ethanol to eliminate ethanol-insoluble FNP from the samples. Quantification of the drug was then performed by measurements of UV absorbance of vinblastine in ethanol solution at 267 nm. The release curve of the drug (Fig. 4a) exhibited slow release kinetics of VIN which lasted for 80 h. This gradual release of the cargo drug is typical for mesoporous silica-based drug carriers and can be described as a two-step process governed by Fickian diffusion of water soluble fullerenol and VIN from the mesopores,[26] which is evident by two linear release tendencies on the Higuchi model plot (Fig. 4a inset). The release kinetics of fullerenol from FAMSN was also demonstrated by measuring its fluorescence at different time points (Fig. S4†).

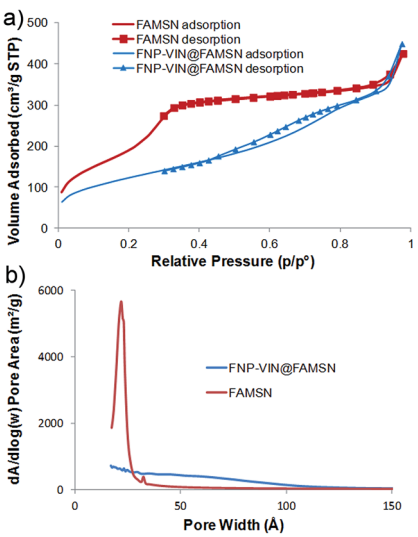

Fig. 3 (a) BET isotherms and (b) BJH calculations for FAMSN and FNP-VIN@FAMSN.

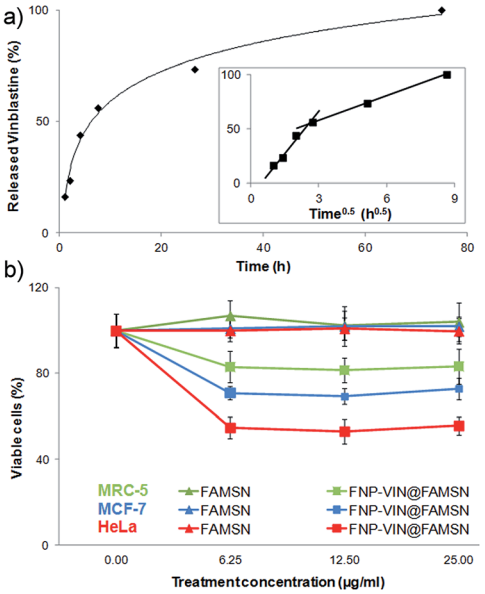

Fig. 4 (a) Release kinetics of vinblastine in PBS from FNP-VIN@FAMSN. Inset shows Higuchi square root of time plot for the release of VIN. (b) Cytotoxicity study on MRC-5, MCF-7 and HeLa cells.

Folate receptor-targeted drug delivery capabilities of the constructed material (FNP-VIN@FAMSN) are further investigated by viability assays on three cell lines: healthy human fetal lung fibroblast cells (MRC-5), MCF-7 breast cancer cells and HeLa cervical cancer cells. These specific cell lines are chosen due to their differences in the amounts of expressed FR. Namely, healthy MRC-5 cells are expected to have the lowest amount of expressed FR,[27] while HeLa cells were already demonstrated to contain much higher amount of expressed FR in comparison to MCF-7 cells.[28] Confocal microscopy studies already revealed the cell internalization capability of FNP,[29,30] while endocytosis of a variety of MSN-based materials have been demonstrated by confocal and TEM imaging.[31] In particular, folic acid-functionalized MSN-based drug delivery systems were demonstrated to undergo endocytosis by clathrin-pitted mechanism,[32] which was also evidenced to enhance in case of increased folate-FR interaction.[33] As can be seen on Fig. 4b the treatments with FNP-VIN@FAMSN showed different potency of the constructed material against the different cell lines, which is exactly in the expected order of efficacy at all employed treatment concentrations, based on the different amounts of expressed folate receptors on the cells' surface. Hence, even at low treatment concentration (6.25 μg mL^{-1}), the activity of FNP-VIN@FAMSN against HeLa cancer cell lines is the highest with 55% of viable cells 24 h after the treatment, while MCF-7 and MRC-5 cells showed 71% and 83% of viable cells, respectively, after the same time period. Thus, we successfully demonstrate that the newly devised nanoconstruct can indeed be utilized for selective treatment of FR-overexpressing cancer cells. This result also showcases that the presence of FNP clusters on the surface of the drug carrier does not hinder the interaction of folate ligands with FR on the cells. No toxic effects were noticed upon the cell treatment with FNP@FAMSN under the same

treatment concentrations (Fig. S5†). Ultimately, this research study points to the applicability of fullerene-based molecules as pore-blockers for construction of MSN-based cancer-targeting drug delivery systems, which opens up a wide range of new research possibilities, *e.g.* to utilize covalently modified fullerenols for construction of different stimuli-responsive drug carriers for simultaneous targeted treatment and diagnostics. The covalent attachment of the fullerenols to the surface of nanoparticles will probably lead to more effective cancer targeting nanotherapeutics as the drug entrapment would be more efficient and "on desire" release of the therapeutic cargo could be enabled through different linking chemistries.

Conclusions

Novel drug delivery system is constructed which contains vinblastine loaded, fullerenol-capped, folic acid-functionalized mesoporous silica nanoparticles. FTIR and TGA measurements confirm the attachment of folic acid on the surface of MSN. Transmission electron microscopy reveals the presence of FNP clusters on the surface of FAMSN while nitrogen sorption and low angle XRD measurements indicate the mesopore-blocking capability of fullerenol. Cell viability studies on healthy MRC-5, breast cancer MCF-7 and cervical cancer HeLa cells reveal the folate receptor-dependent activity of the constructed material and cancer targeting capability of the drug delivery system, which may be applied for selective treatment of tumour tissues.

Acknowledgements

The authors acknowledge the financial support of the Ministry of Education, Science and Technological Development of the Republic of Serbia (grant numbers III45005 and III45019). The ANR (Agence Nationale pour la Recherche, programme Blanc inter I SIMI 10, edition 2012) is gratefully acknowledged. The authors thank T. Cacciaguerra, ICGM France, for the TEM imaging and M. Mitric, Vinca Institute, Serbia, for XRD measurements.

References

1 N. Ž. Knežević and J.-O. Durand, *ChemPlusChem*, 2015, **80**, 26.
2 L. M. Crane, H. J. Arts, M. van Oosten, P. S. Low, A. G. van der Zee, G. M. van Dam and J. Bart, *Cell. Oncol.*, 2012, **35**, 9.
3 Y. Lu and P. S. Low, *Adv. Drug Delivery Rev.*, 2012, **64**, 342.
4 M. Gary-Bobo, O. Hocine, D. Brevet, M. Maynadier, L. Raehm, S. Richeter, V. Charasson, B. Loock, A. Morère, P. Maillard, M. Garcia and J.-O. Durand, *Int. J. Pharm.*, 2012, **423**, 509.
5 P. Saint-Cricq, S. Deshayes, J. I. Zink and A. M. Kasko, *Nanoscale*, 2015, **7**, 13168.
6 N. Z. Knezevic, E. Ruiz-Hernandez, W. E. Hennink and M. Vallet-Regi, *RSC Adv.*, 2013, **3**, 9584–9593.
7 S. Giret, M. Wong Chi Man and C. Carcel, *Chem.–Eur. J.*, 2015, **21**, 13850.
8 M. R. Dzamukova, E. A. Naumenko, Y. M. Lvov and R. F. Fakhrullin, *Sci. Rep.*, 2015, **5**, 10560.
9 P. J. Kempen, S. Greasley, K. A. Parker, J. L. Campbell, H. Y. Chang, J. R. Jones, R. Sinclair, S. S. Gambhir and J. V. Jokerst, *Theranostics*, 2015, **5**, 631.
10 Q. He, Z. Zhang, F. Gao, Y. Li and J. Shi, *Small*, 2011, **7**, 271.
11 J. Lu, M. Liong, Z. Li, J. I. Zink and F. Tamanoi, *Small*, 2010, **6**, 1794.
12 N. Song and Y.-W. Yang, *Chem. Soc. Rev.*, 2015, **44**, 3474.
13 N. Knezevic, S. Milenkovic, D. Jovic, S. Lazarevic, J. Mrdjanovic and A. Djordjevic, *Adv. Mater. Sci. Eng.*, 2015, **2015**, 567350.
14 R. Injac, M. Perse, M. Cerne, N. Potocnik, N. Radic, B. Govedarica, A. Djordjevic, A. Cerar and B. Strukelj, *Biomaterials*, 2009, **30**, 1184.
15 R. Injac, M. Perse, N. Obermajer, V. Djordjevic-Milic, M. Prijatelj, A. Djordjevic, A. Cerar and B. Strukelj, *Biomaterials*, 2008, **29**, 3451.
16 V. Krishna, A. Singh, P. Sharma, N. Iwakuma, Q. Wang, Q. Zhang, J. Knapik, H. Jiang, S. R. Grobmyer, B. Koopman and B. Moudgil, *Small*, 2010, **6**, 2236.
17 J. Grebowski, A. Krokosz, A. Konarska, M. Wolszczak and M. Puchala, *Radiat. Phys. Chem.*, 2014, **103**, 146.
18 P. Chaudhuri, A. Paraskar, S. Soni, R. A. Mashelkar and S. Sengupta, *ACS Nano*, 2009, **3**, 2505.
19 K. D. Pickering and M. R. Wiesner, *Environ. Sci. Technol.*, 2005, **39**, 1359.
20 T. Çavaş, N. Çinkılıç, Ö. Vatan and D. Yılmaz, *Pestic. Biochem. Physiol.*, 2014, **114**, 1.
21 M. Stubbs, P. M. J. McSheehy, J. R. Griffiths and C. L. Bashford, *Mol. Med. Today*, 2000, **6**, 15.
22 A. Djordjević, M. Vojínović-Miloradov, N. Petranović, A. Devečerski, D. Lazar and B. Ribar, *Fullerene Sci. Technol.*, 1998, **6**, 689.
23 S. M. Mirkov, A. N. Djordjevic, N. L. Andric, S. A. Andric, T. S. Kostic, G. M. Bogdanovic, M. B. Vojinovic-Miloradov and R. Z. Kovacevic, *Nitric Oxide*, 2004, **11**, 201.
24 P. Skehan, R. Storeng, D. Scudiero, A. Monks, J. McMahon, D. Vistica, J. T. Warren, H. Bokesch, S. Kenney and M. R. Boyd, *J. Natl. Cancer Inst.*, 1990, **82**, 1107.
25 V. Malgras, Q. Ji, Y. Kamachi, T. Mori, F.-K. Shieh, K. C. W. Wu, K. Ariga and Y. Yamauchi, *Bull. Chem. Soc. Jpn.*, 2015, **88**, 1171.
26 J. Andersson, J. Rosenholm, S. Areva and M. Lindén, *Chem. Mater.*, 2004, **16**, 4160.
27 L. Sun, Y. Zang, M. Sun, H. Wang, X. Zhu, S. Xu, Q. Yang, Y. Li and Y. Shan, *J. Colloid Interface Sci.*, 2010, **350**, 90.
28 D. Feng, Y. Song, W. Shi, X. Li and H. Ma, *Anal. Chem.*, 2013, **85**, 6530.
29 Y. E, L. Bai, L. Fan, M. Han, X. Zhang and S. Yang, *J. Mater. Chem.*, 2011, **21**, 819.
30 J. Jeong, J. Jung, M. Choi, J. W. Kim, S. J. Chung, S. Lim, H. Lee and B. H. Chung, *Adv. Mater.*, 2012, **24**, 1999.
31 Z. Li, J. C. Barnes, A. Bosoy, J. F. Stoddart and J. I. Zink, *Chem. Soc. Rev.*, 2012, **41**, 2590.
32 I. Slowing, B. G. Trewyn and V. S. Y. Lin, *J. Am. Chem. Soc.*, 2006, **128**, 14792.
33 J. Fan, G. Fang, X. Wang, F. Zeng, Y. Xiang and S. Wu, *Nanotechnology*, 2011, **22**, 455102.